FINITE-DIFFERENCE METHODS FOR THE LINEAR ADVECTION EQUATION

Fedor Mesinger

Department of Meteorology, University of Belgrade, Yugoslavia*

*At present, with the Geophysical Fluid Dynamics Program, Princeton University, Princeton, NJ 08540

1. Introduction

This lecture will represent a review of the properties of finite-difference methods used for the linear advection equation

$$\frac{\partial u}{\partial t} + c \frac{\partial u}{\partial x} = 0; \qquad c = \text{const.} \tag{1.1}$$

Here $u(x,t)$ is a function of two independent variables; the independent variable x will represent a space variable, and t time. Thus, (1.1) will represent a one-dimensional linear advection equation. Generalizations to two space dimensions shall not be included, since no fundamental problems have been noticed to arise in such generalizations.

It is now widely understood that the main computational problems in the finite-difference solution of (1.1) are those encountered due to space differencing. Thus, these problems will be outlined first; they are the problems of the phase speed error and of the computational dispersion. Subsequently, the effect of time differencing shall be analyzed.

Finite difference treatment of the linear advection equation is a standard introductory subject of all review texts on difference methods used in atmospheric models. As probably the most recent widely available text, the book by Haltiner and Williams (1980) can be mentioned. In this lecture, I shall, for a presentation of the mentioned space differencing problems, follow the earlier monograph by Mesinger and Arakawa (1976). The analysis of the effect of time differencing will be based mostly on a recent manuscript by Takacs (1984). The subject of the linear advection equation will receive additional coverage in some of the following lectures.

2. Centered second-order space differencing: phase speed error and computational dispersion

If the x axis is divided into equal space increments, and the space derivative in (1.1) then approximated by a centered finite difference quotient using values at the two nearest points, we obtain for the time derivative

$$\frac{\partial u_j}{\partial t} = -c\frac{u_{j+1} - u_{j-1}}{2\Delta x}. \tag{2.1}$$

The subscript here denotes the distance from the origin in space increments; that is, $x = j\Delta x$. We now want to have a look at the properties of (2.1) which are due to the space differencing it contains. The solution of (1.1) being known, a most logical and also a feasible way at our disposal is a comparison of the solutions of (2.1) against those of the differential equation it approximates.

In this situation, it is generally found most instructive to consider the solution in form of a single harmonic component

$$u(x,t) = \mathrm{Re}\left[U(t)e^{ikx}\right]. \tag{2.2}$$

Inserting (2.2) into (1.1), we find that it is indeed a solution of the considered advection equation, provided that

$$\frac{dU}{dt} + ikcU = 0. \tag{2.3}$$

In this oscillation equation, kc is equal to the frequency ν, and $c = \nu/k$ is the phase speed of the waves. It is seen that waves of all wave lengths are propagated with the same phase speed, that is, the function u(x,t) is advected with no change in shape at a constant velocity c along the x axis. There is no dispersion.

For the solution of (2.1), we insert

$$u_j(t) = \mathrm{Re}\left[U(t)e^{ikj\Delta x}\right], \tag{2.4}$$

which results in

$$\frac{dU}{dt} + ik\left(c\frac{\sin k\Delta x}{k\Delta x}\right)U = 0. \tag{2.5}$$

Thus, instead of the constant phase speed c, we see that waves now propagate with the phase speed

$$c^* = c\,\frac{\sin k\Delta x}{k\Delta x} \tag{2.6}$$

This phase speed is a function of the wave number k. Thus, the finite differencing in space causes a dispersion of the waves; this effect is called computational dispersion. As $k\Delta x$ increases from zero, the phase speed c* monitonically decreases from c, and becomes zero for the shortest resolvable wave length $2\Delta x$, when $k\Delta x = \pi$. Thus, all waves propagate at a speed that is less than the true phase speed c, with this decelerating effect increasing as the wave length decreases. The two-grid-interval wave is stationary.

The reason for the two-grid-interval wave being stationary is obvious when we look at the plot of that wave, shown in Fig. 2.1. For this wave $u_{j+1} = u_{j-1}$ at all grid points, and (2.1) gives a zero value for $\frac{\partial u_j}{\partial t}$.

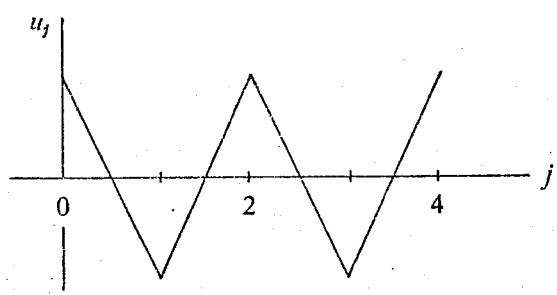

Figure 2.1. A plot of the "two-grid-interval" wave, with a wave length of $2\Delta x$.

We have encountered two effects here. Firstly, the advection speed is less than the true advection speed. The consequence of this error is a general retardation of the advection process. Secondly, the advection speed changes with wave number; this false dispersion is particularly serious for the shortest waves.

We now turn our attention to the group velocity. In the case of the linear equation (1.1), we obtain for the group velocity c_g

$$c_g = \frac{d(kc)}{dk} = c. \tag{2.7}$$

Thus, the group velocity is constant and equal to the phase speed c. With the differential-difference equation (2.1), however, (2.6) gives for the group velocity

$$c_g^* = \frac{d(kc^*)}{dk} = c \cos k\Delta x. \tag{2.8}$$

Thus, as $k\Delta x$ increases from zero, the group velocity c_g^* decreases monotonically from c_g, and becomes equal to $-c_g$ for the shortest resolvable wave length of $2\Delta x$.

These results are summarized in Fig. 2.2. For the exact advection equation (1.1) both individual waves and wave packets (that is places where superposition of waves results in a maximum amplitude of a group of neighboring wave numbers) propagate at the same constant velocity $c = c_g$. Introduction of the centered difference quotient in (2.1) makes both the phase speed and the group velocity decrease as the wave number increases. The error is particularly great for the shortest resolvable wave lengths; waves with wave lengths less

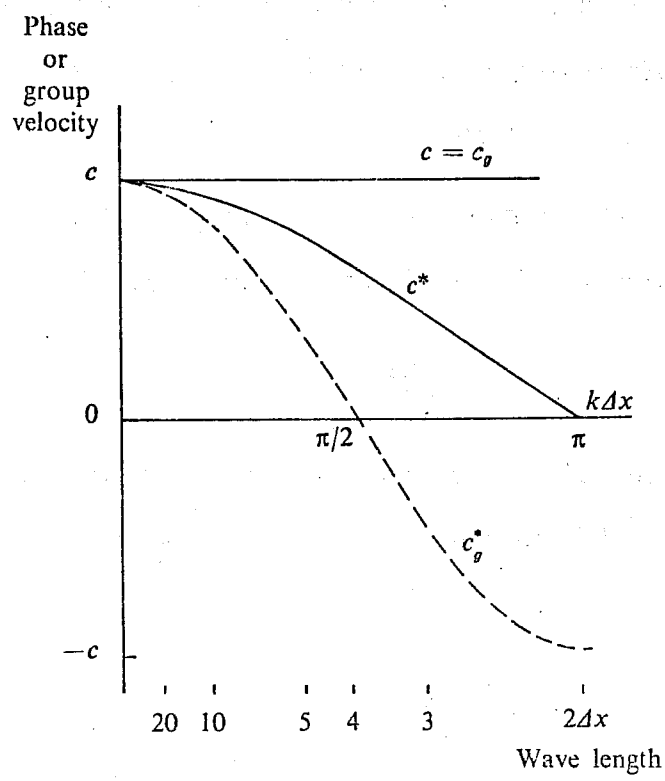

Figure 2.2. Phase speed and group velocity, in the case of the linear advection equation, c and c_g, and in the case of the corresponding differential-difference equation with second-order centered space differencing, c* and c_g^* (Matsuno, 1966).

than $4\Delta x$ even have a negative group velocity. This means that wave packets made up of these waves propagate in the direction opposite to the advection velocity and opposite to the direction of propagation of individual waves.

It is possible to obtain an analytic solution of (2.1), which can be used to analyze its behavior for some given initial conditions of interest. To this end, it is convenient to define a non-dimensional time variable

$$\tau \equiv ct/\Delta x,$$

and, after dividing (2.1) by $c/2\Delta x$, to write it in the form

$$2\frac{d}{d\tau}u_j(\tau) = u_{j-1}(\tau)-u_{j+1}(\tau). \qquad (2.9)$$

This can be recognized as the recurrence formula of the Bessel function of the first kind of order j, $J_j(\tau)$. In other words,

$$u_j(\tau) = J_j(\tau), \qquad (2.10)$$

is a solution of (2.9). Several of these functions, of the lowest order, are shown in Fig. 2.3. The figure illustrates more of these functions than indicated, since, for any j,

$$J_{-j} = (-1)^j J_j.$$

Note, furthermore, that in (2.9) the subscript j can take any integer value, since the location of the grid point for which we choose j = 0 is arbitrary. Thus, a solution that is more general than (2.10) is

$$u_j(\tau) = J_{j-p}(\tau),$$

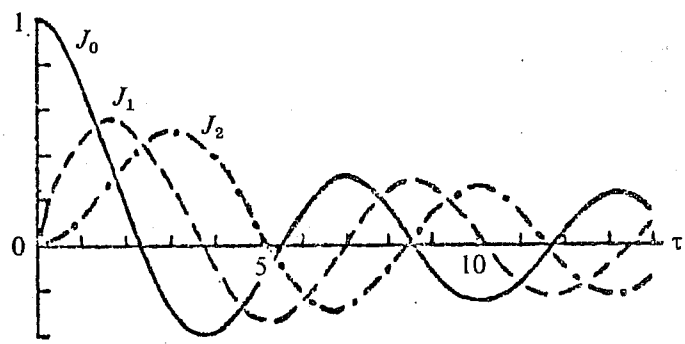

Figure 2.3. The Bessel functions $J_0(\tau)$, $J_1(\tau)$ and $J_2(\tau)$.

where p is an arbitrary integer. A still more general solution is a linear combination of all these solutions, that is

$$u_j(\tau) = \sum_{p=-\infty}^{\infty} a_p \, J_{j-p}(\tau), \qquad (2.11)$$

where a_p are arbitrary constants. Now, for $\tau = 0$ all of the functions J_k are equal to zero, except J_0, for which $J_0(0) = 1$. Hence, substituting $\tau = 0$ into (2.11) we obtain

$$u_j(0) = a_j. \qquad (2.12)$$

Therefore the constants in (2.11) can be chosen so as to satisfy arbitrary initial conditions $u_j = u_j(0)$. In this way, (2.11) is seen to represent the general solution of (2.9), or (2.1).

It is instructive to look in some detail at the solution satisfying the initial conditions

$$u_j(0) = \begin{cases} 1 & \text{for } j=0 \\ 0 & \text{for } j\neq 0 \end{cases} \qquad (2.13)$$

the simplest solution of the form (2.10), for different values of the non-dimensional time. At the initial moment the function u_j consists of a single pulse-like disturbance centered at the point $j = 0$, as shown in the upper diagram of Fig. 2.4. We note that, because of (2.9), $du_j/d\tau$ is then equal to zero at all points except at $j = -1$ and $j = 1$, where it is equal to $-1/2$ and $1/2$, respectively.

Thus, at the initial moment the disturbance propagates at the same rate in the directions of both the positive and the negative x axis. Further propagation of the disturbance can be followed by the evaluation

of (2.10) for various times; solutions obtained for $\tau = 5$ and $\tau = 10$ are shown in the middle and lower diagrams of Fig. 2.4, respectively.

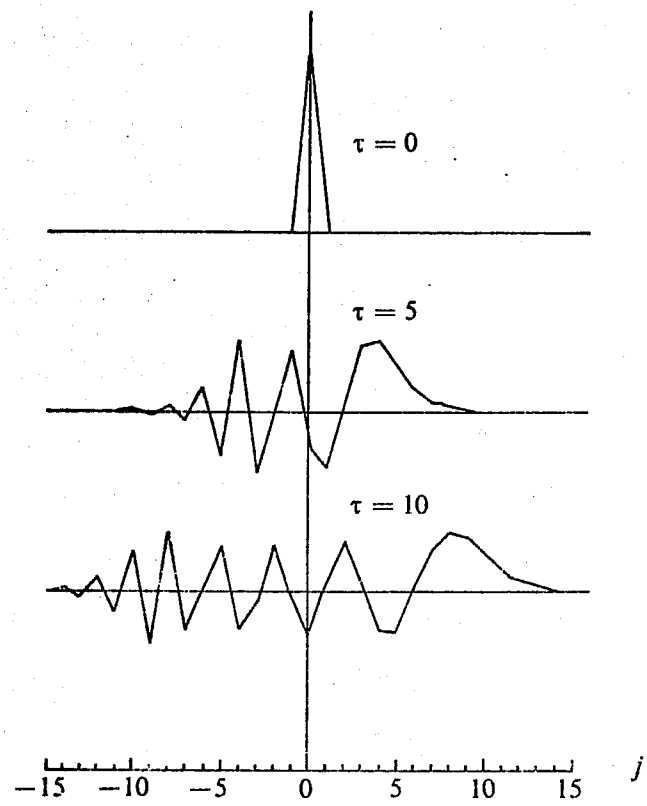

Figure 2.4. The analytic solution of (2.1), for the initial conditions shown in the uppermost of the three diagrams, for two subsequent values of the non-dimensional time τ (Matsuno, 1966).

The three diagrams present an example of the computational dispersion of the second-order centered space differencing. Expansion of a single grid point pulse-like disturbance as a cosine Fourier integral shows that it consists of all harmonic components, present with an equal amplitude. According to Fig. 2.2, its various Fourier components are advected with different phase speeds, bringing about a dispersion of the disturbance. With the non-dimensional time chosen here, we see from (2.9) that the physical advection velocity should keep the pulse located at the point $j = \tau$. Because of the space difference approximation, however, all the phase speeds are less than the physical advection velocity. The main disturbance, as seen in Fig. 2.4, is advected at a speed only slightly less than the physical one; obviously it is formed mostly of the longer wave components, which have an advection speed not much different from the physical advection velocity. However, it is seen to be diffusing away with time, which is again a result of the dispersion. We also observe propagation of a group of short waves in the direction opposite to that of the physical advection. Since the appearance of these waves contradicts the physical properties of the advection equation, such waves are called parasitic waves.

For a more satisfactory difference solution in the case of pulse-like initial condition, with no change in the scheme used, of course more grid points across the disturbance are needed. Rather than looking at results which can be achieved in this way at this point, it is more appropriate to analyze properties of other difference approximations that may appear attractive for the solution of (1.1).

3. Upstream first-order space differencing

With the considered initial condition, obviously, no parasitic waves can be created when using the upstream scheme for the space derivative

$$\frac{\partial u_j}{\partial t} + C \frac{u_j - u_{j-1}}{\Delta x} = 0, \text{ for } C > 0. \qquad (3.1)$$

This choice is certainly appealing from the point of view of the direction of the propagation of the disturbance according to the differential equation we want to approximate.

The analytic solution of (3.1) can be obtained in a manner entirely analogous to that just used in the case of centered differencing. As the solution satisfying the single grid point pulse-like initial condition of the preceding section, one obtains the Poisson frequency function

$$u_j(\tau) = \begin{cases} \dfrac{c^{-\tau}\tau^{j-p}}{(j-p)!} & \text{for } j \geq p, \\ 0 & \text{for } j < p \end{cases} \qquad (3.2)$$

This being a frequency function, it encloses an area equal to unity for all values of . As the non-dimensional time τ increases, the shape of the histogram defined by (3.2) changes in such a way as to have its mean position

$$\sum_{j-p=0}^{\infty} (j-p) \frac{c^{-\tau}\tau^{j-p}}{(j-p)!} = \tau$$

move at a constant speed, equal to the physical advection velocity. Finally, during this advection process, no false negative values are created.

A linear combination of all possible solutions (3.2)

$$u_j(\tau) = \sum_{p=-\infty}^{j} a_p \frac{e^{-\tau}\tau^{j-p}}{(j-p)!} \tag{3.3}$$

for $\tau = 0$ reduces to

$$u_j(0) = a_j$$

Thus, this is the general solution of (3.1).

An example of the solutions (2.11), for centered differencing, and (3.3), for upstream differencing, for the initial disturbance

$$u_j(0) = \begin{cases} 1 & \text{for } j = -1,0,1 \\ 0 & \text{for } j \neq -1,0,1 \end{cases}$$

is shown in Fig. 3.1. If the grid distance is of the order of 150 km, and c is about 15 ms^{-1}, we can see that

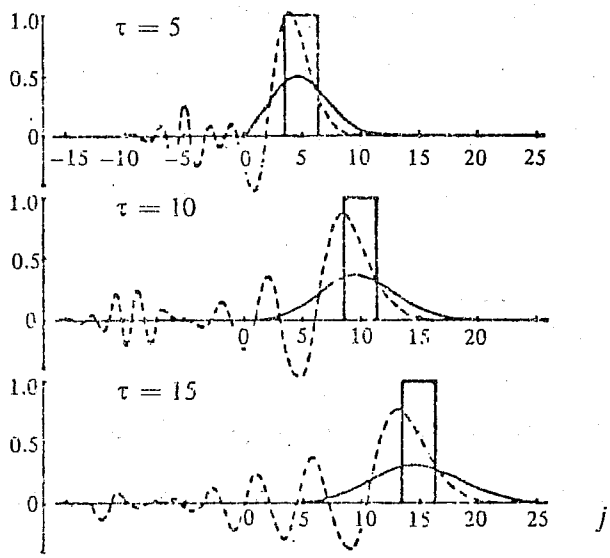

Figure 3.1. Analytic solutions of the exact advection equation (heavy solid line), of the equation using centered differencing (dashed line), and of the equation using upstream differencing (thin solid line), for three different values of the non-dimensional time τ (Wurtele, 1961).

10 units of non-dimensional time approximately correspond to the physical time of one day. Thus the damping effect of the first-order upstream differencing is seen to be quite severe.

4. Centered fourth-order space differencing

An alternative attempt to explore the possibilities for an improvement in the overall properties of the difference solution can be made by increasing the order of accuracy of the space differencing. The simplest way of achieving a higher order accuracy is the use of the fourth-order accurate "four thirds minus one third" approximation to the space derivative. This results in the scheme

$$\frac{\partial u_j}{\partial t} + c\left(\frac{4}{3}\,\frac{u_{j+1} - u_{j-1}}{2\Delta x} - \frac{1}{3}\,\frac{u_{j+2} - u_{j-2}}{4\Delta x}\right) = 0 \tag{4.1}$$

Inserting here a tentative solution in form of a single harmonic component, (2.4), we find the phase speed

$$c^{**} = c\left(\frac{4}{3}\,\frac{\sin k\Delta x}{k\Delta x} - \frac{1}{3}\,\frac{\sin 2k\Delta x}{2k\Delta x}\right) \tag{4.2}$$

This phase speed as a function of $k\Delta x$, along with that obtained with second-order centered differencing, is shown in Fig. 4.1. The figure illustrates the very substantial increase in accuracy of the phase speed for large-scale and medium-scale waves. However, as the wave length approaches its minimum value of $2\Delta x$, the increase in phase speed obtained by fourth order differencing diminishes, until, finally, the wave with wave length $2\Delta x$ is again stationary.

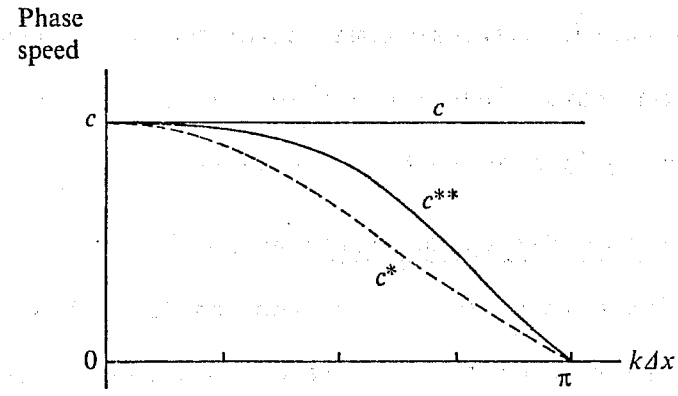

Figure 4.1 Phase speed for the linear advection equation, c, and for the corresponding differential-difference equations with second order (c*) and with fourth order (c**) centered space differencing.

Moreover, for short waves the slope of the phase speed curve is greater than with second-order differencing, and, therefore, the computational dispersion of these waves is greater.

The group velocity resulting from (4.2) also shows a substantial improvement for longer waves. Some improvement is also achieved for medium-scale waves, so that the region of negative group velocities is reduced. The shortest waves, however, have a larger group velocity error than with second-order differencing.

5. Explicit two-level time differencing

While all of the features considered so far are important and may and/or have been the subject of special additional efforts, the issue of the phase speed accuracy stands out as the dominant issue of the linear advection equation schemes used in finite-difference weather prediction models. Thus, significant improvements have been reported in the performance of comprehensive atmospheric models resulting from the use of fourth-order schemes for the horizontal advection or for all space derivative terms. Nevertheless, the systematic phase speed retardation due to space differencing has remained a matter of much concern.

A simple possibility to improve the situation is offered by time differencing. Time differencing can have an accelerating effect, and thus, under favorable circumstances, can alleviate the phase speed problem due to space differencing. This is the basis of numerous efforts in constructing difference schemes for the linear advection equation, with results published in meteorological (e.g., Crowley, 1968; Molenkamp, 1968; Anderson and Fattahi, 1974) as well as other literature. We shall here, following a manuscript by Takacs (1984), present a systematic analysis of the situation arising when an explicit and two time level scheme is used for the time derivative. This can be considered as the simplest class of time differencing schemes; with attractive features of the least possible storage requirements, and of the absence of the time computational mode.

For a general approach, we consider the scheme

$$u_j^{n+1} \sum_p a_p u_{j+p}^n , \quad p = 0, \pm 1, \pm 2, \ldots, \tag{5.1}$$

with superscripts denoting the time level of the difference variable, and a_p the coefficients defining the scheme.

Conditions can be imposed on the coefficients a_p necessary to satisfy a desired set of requirements. By the Taylor series expansion about the joint $j\Delta x, n\Delta t$, it can be shown that for the first-order accuracy, in both space and time, we need

$$\sum_p a_p = 1, \qquad \sum_p p a_p = -\mu, \tag{5.2}$$

where μ is the Courant-Friedrichs-Lewy (CFL) stability parameter

$$\mu \equiv \frac{c\Delta t}{\Delta x}$$

Second-order accuracy, in addition to (5.2), requires

$$\sum_p p^2 a_p = \mu^2 \tag{5.3}$$

For mth-order accuracy, there are m+1 requirements, beginning with (5.2) and ending with

$$\sum_p p^m a_p = (-\mu)^m \tag{5.4}$$

A scheme satisfying the requirements (5.2) through (5.4) is mth-order accurace in both space and time. A familiar example is the second-order accurate Lax-Wendroff scheme.

Some insight into the properties of (5.1), as a function of the number of accuracy requirements satisfied, can be gained by a comparison of its wave solution against that of the continuous equation. For a wave solution of (5.1) we insert

$$u_j^n = \mathrm{Re}\left(\hat{u}^n e^{ikj\Delta x}\right) \tag{5.5}$$

defining, at the same time,

$$\hat{u}^{n+1} \equiv \lambda \hat{u}^n \ ; \qquad \lambda \equiv \mathrm{Re}^{i\phi}$$

we obtain

$$\mathrm{Re}^{i\phi} = \sum_p a_p e^{ikp\Delta x} \tag{5.6}$$

Introducing, for brevity, the non-dimensional wave number

$$\theta \equiv k\Delta x,$$

this can be written as

$$R = \left[\left(\sum_p a_p \cos p\theta\right)^2 + \left(\sum_p a_p \sin p\theta\right)^2\right]^{\frac{1}{2}}$$

$$\phi = \tan^{-1}\left[\left(\sum_p a_p \sin p\theta\right) / \left(\sum_p a_p \cos p\theta\right)\right] \tag{5.7}$$

On the other hand, the wave solution of the continuous equation can be written in the form

$$u_T(x,t) = \mathrm{Re}\left[R^{t/\Delta t}\hat{u}(o)e^{\,i(kx+\phi t/\Delta t)}\right] \tag{5.8}$$

with

$$R_T = 1, \quad \Phi_T = -\mu\theta, \tag{5.9}$$

representing the amplitude amplification factor, and phase change per time step, respectively, of the true solution.

For a comparison of (5.7) and (5.9), R and ϕ being wave number dependent can now be expanded into Taylor series about $\theta = 0$. The true solution gives

$$R_{T_o} = 1,$$

$$\left(d^M R_T/d\theta^M\right)_o = 0, \qquad M = 1,2,3\ldots\ , \tag{5.10}$$

and

$$\phi_{T_o} = 0,$$

$$\left(d^N \phi_T/d\theta^N\right)_o = \begin{cases} -\mu, & N = 1 \\ 0, & N = 2,3,4,\ldots\ , \end{cases} \tag{5.11}$$

with subscripts 0 denoting values at $\theta = 0$. The discrete solution, however, results in

$$R_o = \sum_p a_p$$

$$\left(d^M R/d\theta^M\right)_o = 0, \qquad M = 1,3,\ldots\ , \tag{5.12}$$

and

$$\phi_o = 0,$$

$$(d^N\phi/d\theta^N)_o = \begin{cases} \sum_p pa_p / \sum_p a_p, & N = 1 \\ 0, & N = 2,4,\ldots \end{cases} \qquad (5.13)$$

For even derivatives of R and odd derivatives of ϕ complicated expressions are obtained, involving the coefficients a_p. It can be shown (Takacs, personal communication) that by choosing the coefficients following the order of accuracy requirements more and more derivatives of R and ϕ can be made to vanish. This is summarized in Table 1. The table supports the impression that may have been obtained from a comparison of the results of the preceding sections, in that improvements in the amplitude properties of the scheme can be obtained by going for an

Order of accuracy	Minimum number of grid points needed	Amplitude conditions satisfied: $R_o = 1$, and $(d^{M'}R/d\theta^{M'})_o = 0$ for $M' = M,1,3,\ldots$	Phase conditions satisfied: $(d\phi/d\theta)_o = -\mu$, and $(d^{N'}\phi/d\theta^{N'})_o = 0$ for $N' = N,2,4,\ldots$
1	2		
2	3	M = 2	
3	4	M = 2	N = 3
4	5	M = 2,4	N = 3
5	6	M = 2,4	N = 3,5
	. . .		

Table 1 Amplitude amplification and phase characteristics of two time level schemes as a function of the order of accuracy.

odd to the next higher even-ordered scheme, while improvements in the phase properties can be achieved by going from an even to the next higher odd-ordered scheme.

However, given the number of grid points one is considering for use within the advection scheme, it does not necessarily follow that satisfying the maximum number of the order of accuracy requirements should give the best result. For an analysis of this issue, we again follow Takacs (1984), in considering the case of the four point scheme. With three points centered and the fourth point upstream (p = 1,0,-1,-2), Takacs has chosen to

i) impose the second order accuracy requirements;

ii) have the coefficient of the extra upstream point depend on μ so that for $\mu = 0$ or 1 the scheme is exact;

iii) impose an additional restriction on this coefficient requiring that the scheme be stable;

(iv) make an experimental study of this family of stable schemes with a view to minimizing some measure of error.

Step i) of this procedure restricts analysis to the scheme

$$u_j^{n+1} = a_1 u_{j+1}^n + a_o u_j^n + a_{-1} u_{j-1}^n + a_{-2} u_{j-2}^n \; ; \qquad (5.14)$$

$$a_1 = \mu(\mu-1)/2 - a_{-2} \; ,$$

$$a_o = 1 - \mu^2 + 3a_{-2} \; ,$$

$$a_{-1} = \mu\,(\mu+1)/2 - 3a_{-2} \; .$$

The requirement of step ii) is achieved by

$$a_{-2} = \alpha\mu(\mu-1). \tag{5.15}$$

The stability restriction of step iii) is found to be

$$0 \leqq \alpha \leqq 1/2. \tag{5.16}$$

Within this range, for $\alpha = (\mu + 1)/6$, the scheme becomes third-order accurate; and for $\alpha = 0.25$, it reduces to the "zero average phase speed error scheme" of Fromm.

As step iv), Takacs has performed and analyzed experiments similar to those of a number of previous studies: a cone-shaped disturbance, of a base-width of 10 grid points, was advected over a distance of 70 grid points. This initial condition, at the same time the true solution at the verification time, is shown in Fig. 5.1. Three error measurements

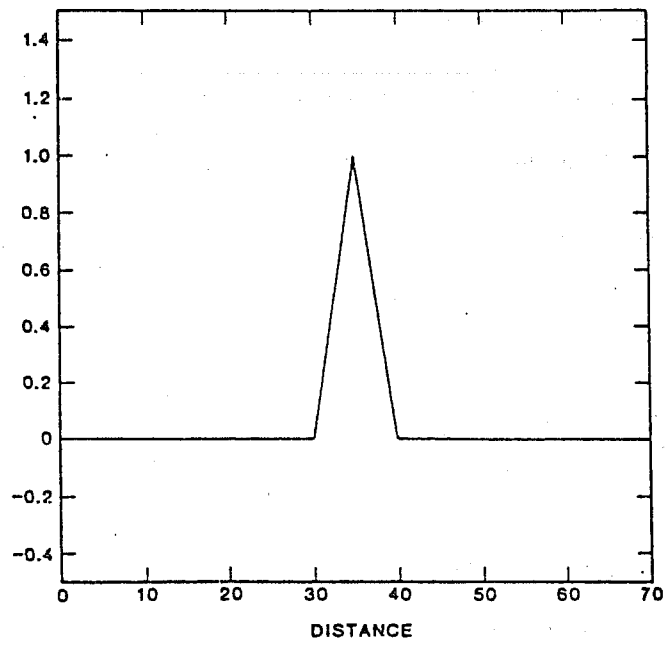

Figure 5.1. The initial condition of Takacs' one-dimensional advection experiments.

were taken; one was the MS error, called the total error,

$$E_{TOT} \equiv \overline{(u_T - u_j)^2} \tag{5.17}$$

The bar here denotes the arithmetic average over all the 70 grid points. A straightforward manipulation of (5.17) leads to

$$E_{TOT} = [\sigma(u_T) - \sigma(u_j)]^2 + (\bar{u}_T - \bar{u}_j)^2 + 2(1-\rho)\,\sigma(u_T)\,\sigma(u_j), \tag{5.18}$$

where σ^2 represents the variance of a quantity, and ρ the correlation coefficient of u_T and u_j. Thus, if u_T and u_j are exactly correlated, all of the considered error will be contained in the first two terms of the right-hand side of (5.18). Takacs, therefore, defines the sum of these two terms to represent the "dissipation error"

$$E_{DISS} \equiv [\sigma(u_T) - \sigma(u_j)]^2 + (\bar{u}_T - \bar{u}_j)^2 \tag{5.19}$$

and the third term, present only for $\rho \neq 1$, the "dispersion error"

$$E_{DISP} \equiv 2(1-\rho)\,\sigma(u_T)\,\sigma(u_j). \tag{5.20}$$

The three error measurements obtained in advection experiments for various values of α and μ are shown in Fig. 5.2. The numbers in the figure are scaled by the maximum MS error, and by the number of time steps required to advect the cone the 70 grid point distance. Thus, these are errors per time step, as functions of the scheme, and the Courant number used.

Minimization of the total error is seen to occur along the third-order accuracy line. Compared to the Lax-Wendroff scheme ($\alpha = 0$) the extra grid point can substantially reduce the total error. Dissipation errors obtained are about an order of magnitude smaller than the total error.

They are not much affected by the extra point added to the second-order scheme. Reduction of the total error thus, to a very large extent, represents the reduction of the dispersion error. Note that, for the third-order scheme, this should have been anticipated on the basis of results shown in Table 1.

The appropriate choice of α in a comprehensive atmospheric model apparently depends on the effective Courant number used. Explicit time differencing in grid point models tends more and more to be associated with splitting, so that large time steps are used for advection steps. The value of $\alpha = 0.25$ then may be appropriate. With no splitting and small effective Courant numbers, a smaller value should be better.

Results of experiments performed by Takacs in which the initial condition of Fig. 5.1 was advected two translations over the 70 grid point domain are shown in Fig. 5.2. Fig. 5.3 shows the results obtained for $\mu = 0.2$, and Fig. 5.4 those for $\mu = 0.7$. In each figure, results are shown obtained using the first-order forward-upstream scheme (panel a), Lax-Wendroff scheme (b), considered four-point scheme with $\alpha = 0.20$ (c), Fromm scheme, obtained for $\alpha = 0.25$ (d), fourth-order space differencing with leapfrog time differencing (e), and the third-order scheme (f). Note that for $\mu = 0.2$, the four-point scheme with $\alpha = 0.2$ is, in fact, the third-order accurate scheme. In each plot, the total error, dissipation error, and dispersion error, as defined previously, are also presented; again scaled by the total number of time steps.

The phase error problem of the second-order scheme is indeed seen to be eliminated to a very large extent by going to the four-point schemes. The Fromm scheme for $\mu = 0.2$ has even resulted in

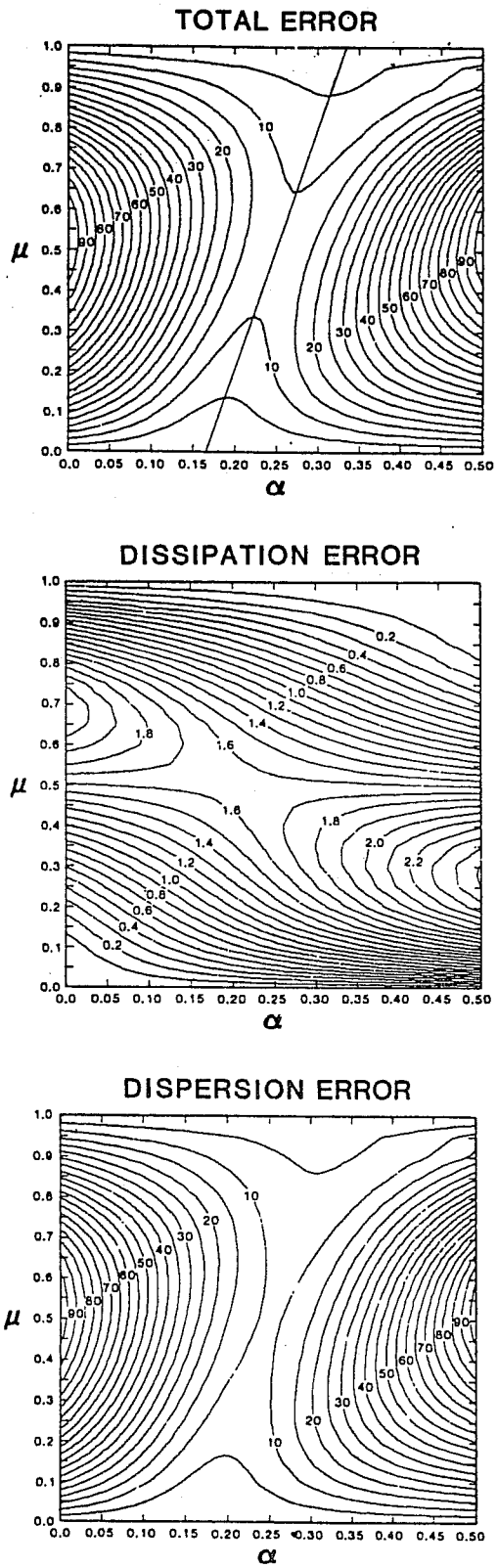

Figure 5.2. Total MS error, dissipation and dispersion error as defined by (5.19) and (5.20), respectively, per time step, and in percents of the maximum MS error. Values are obtained after advecting the initial condition of Fig. 5.1 over a distance of 70 grid points. The straight line in the upper panel shows the third-order accurate scheme. (Takacs, 1984).

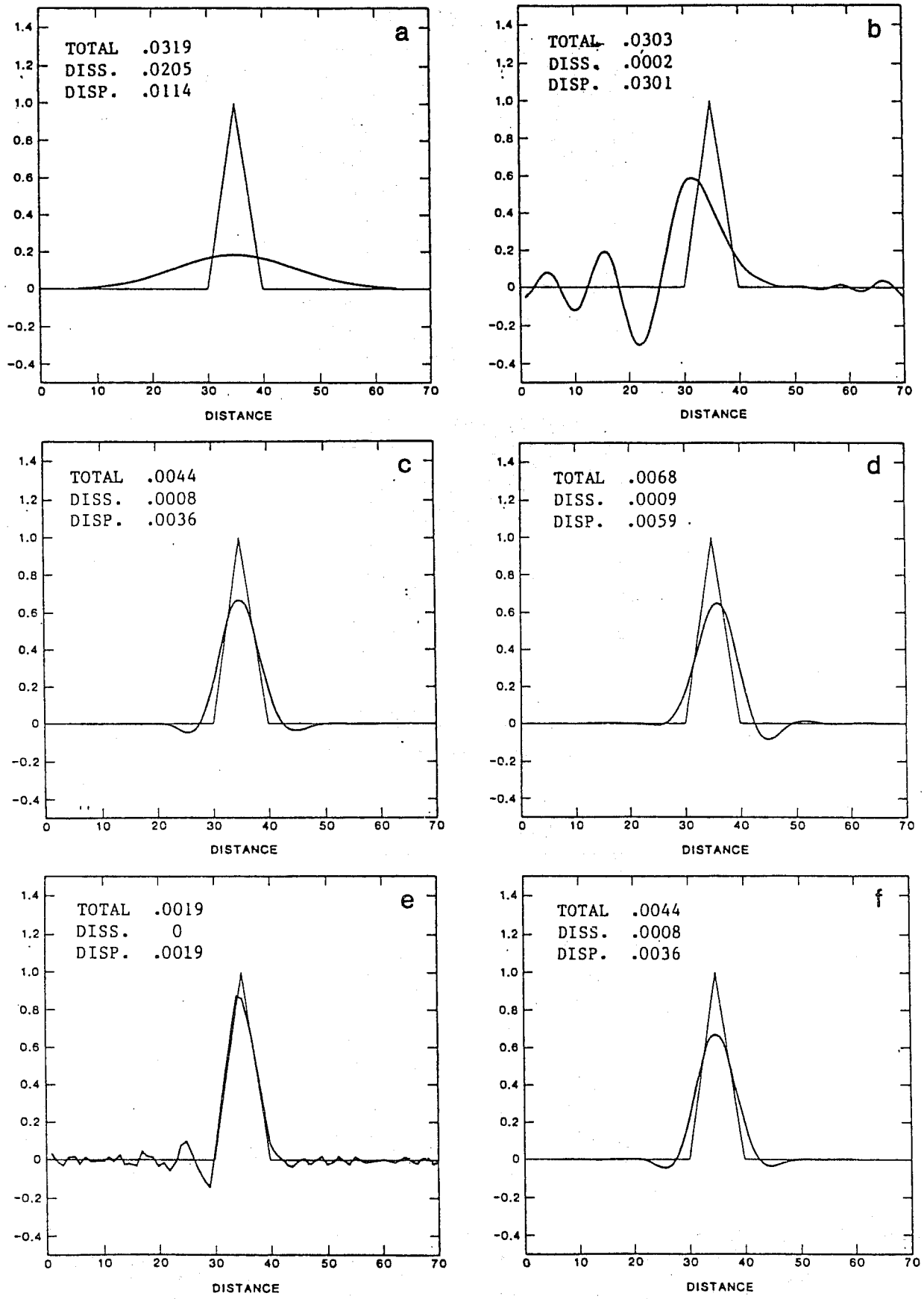

Fig. 5.3. One-dimensional advection experiments, for $\mu = 0.2$. See text for details. (Takacs, 1984).

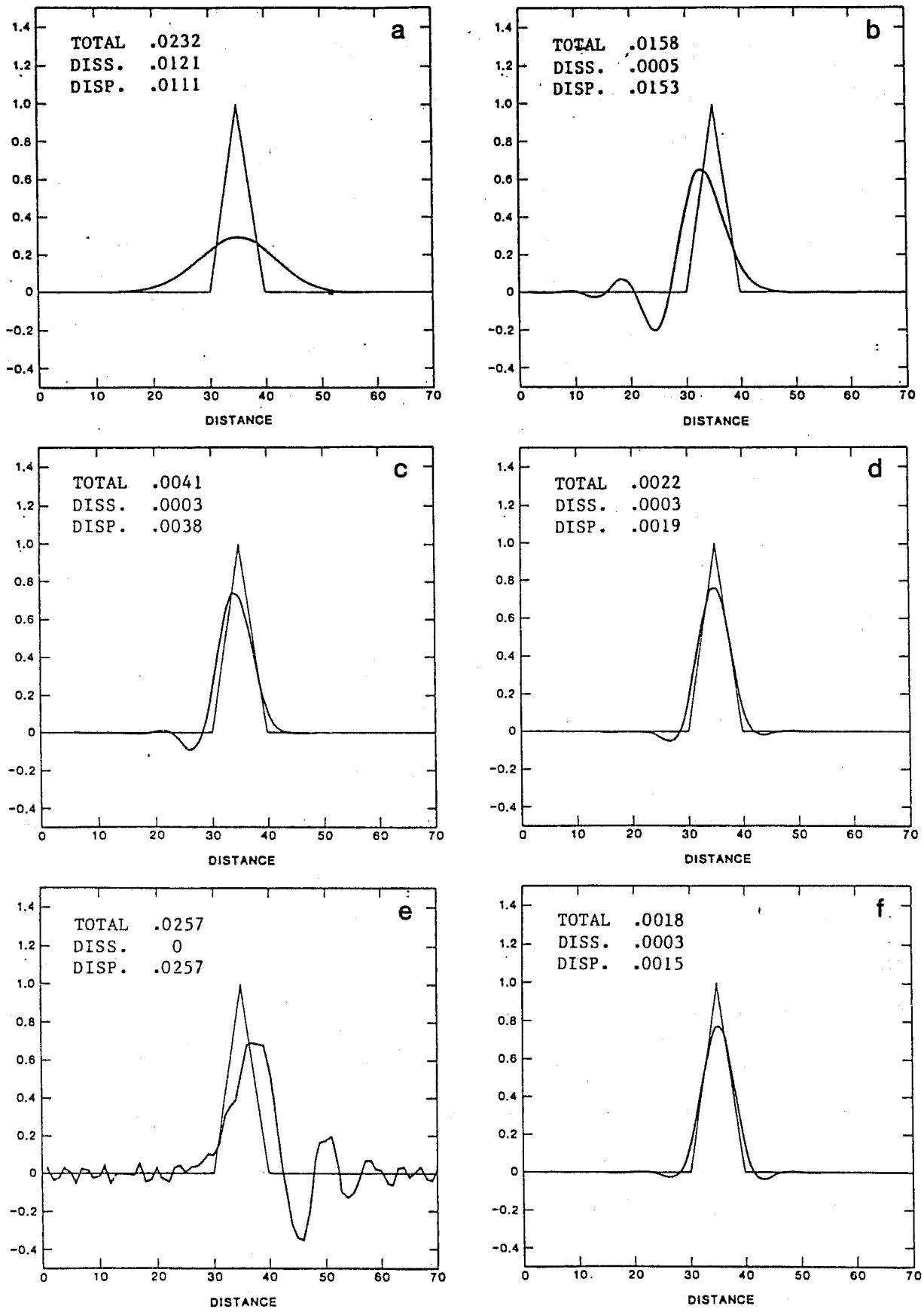

Fig. 5.4. One-dimensional advection experiments, for $\mu = 0.7$. See text for details. (Takacs, 1984)

an advection of the main disturbance faster than that of the true solution. This has occurred also in the case of the space fourth-order accurate scheme for $\mu = 0.7$, but at the cost of a much too large dispersion error. A scheme with some dissipation, such as that developed by Gadd (1978) might have given a better result in that case.

For results of additional experiments, including consideration of the two-dimensional case, the reader is referred to the paper by Takacs (1984).

6. Concluding remarks

The subject of the finite-difference solution of the linear advection equation is a vast research area, of interest in many fields of fluid dynamics. Thus, many more techniques have been developed than has been possible to review in this introductory lecture. In addition to the phase speed objective, techniques have been developed also aimed at preserving other special features of various fluid dynamics problems. As an example, the problem of advecting a non-negative quantity can be mentioned (e.g., water vapor, thickness of potential temperature layers in isentropic coordinate models); or that of preserving a discrete analog of an integral quantity considered to be of importance for an advection problem. For additional reading on these and other techniques, the reader is referred to Smolarkiewicz (1983); Arakawa and Lamb (1977); to related lectures published in the present volume, and to papers on advection equation methods published in proceedings of the 1983 AMS-SIAM Summer Seminar on Large-Scale Computations in Fluid Mechanics, in American Mathematical Society's series Lectures in Applied Mathematics, 1984. Finally, the

finite element as well as spectral methods can and are successfully used for the linear advection equation, as also discussed in other lectures in the present volume.

Acknowledgement

I am grateful to Mr. Lawrence Takacs, of the Goddard Laboratory for Atmospheric Sciences, NASA/Goddard Space Flight Center, for supplying me with an unpublished manuscript which I have summarized within Section 5 of this lecture.

REFERENCES

Anderson, D., and B. Fattahi, 1974: A comparison of numerical solutions of the advection equation. J. Atmos. Sci., 31, 1500-1506.

Arakawa, A., and V.R. Lamb, 1977: Computational design of the basic dynamical processes of the UCLA general circulation model. Methods in Computational Physics, Vol. 17, General Circulation Models of the Atmosphere, J. Chang, Ed., Academic Press, 173-265.

Crowley, W.P., 1968: Numerical advection experiments. Mon. Wea. Rev., 96, 1-11.

Gadd, A.J., 1978: A numerical advection scheme with small phase speed errors. Quart. J. Roy Meteor. Soc., 104, 583-594.

Haltiner, G.J., and R.T. Williams, 1980: Numerical Prediction and Dynamic Meteorology. Second Edition. Wiley, New York. 478 pp.

Matsuno, T., 1966: False reflection of waves at the boundary due to the use of finite differences. J. Meteor. Soc. Japan, Ser. 2, 44, 145-157.

Mesinger, F., and A. Arakawa, 1976: Finite difference schemes used in atmospheric models, Vol. I. GARP Publ. Ser., No. 17, WMO, Geneva, 64 pp.

Molenkamp, C.R., 1968: Accuracy of finite difference methods applied to the advection equation. J. Appl. Meteor., 7, 160-167.

Smolarkiewicz, P.K., 1983: A simple positive definite advection scheme with small implicit diffusion. Mon. Wea. Rev., 111, 479-486.

Takacs, L.L., 1984: Empirically derived second-order schemes for the advection equation with minimum dissipation and dispersion errors. Submitted to Mon. Wea. Rev.

Wurtele, M.G., 1961: On the problem of truncation error. Tellus, 13, 379-391.